International Journal of Pharmaceutics 513 (2016) 473–482

Contents lists available at ScienceDirect

International Journal of Pharmaceutics

journal homepage: www.elsevier.com/locate/ijpharm

Gelatin-based membrane containing usnic acid-loaded liposome improves dermal burn healing in a porcine model

Paula Santos Nunes, Prof.[a,*], Alessandra Silva Rabelo[b], Jamille Cristina Campos de Souza[b], Bruno Vasconcelos Santana[b], Thailson Monteiro Menezes da Silva[b], Mairim Russo Serafini[b], Paula dos Passos Menezes[b], Bruno dos Santos Lima[b], Juliana Cordeiro Cardoso[c], Júlio César Santana Alves[d], Luiza Abrahão Frank[e], Sílvia Stanisçuaski Guterres[e], Adriana Raffin Pohlmann[e], Malone Santos Pinheiro[c], Ricardo Luiz Cavalcanti de Albuquerque Júnior[c], Adriano Antunes de Souza Araújo[b]

[a] Department of Morphology, Federal University of Sergipe, Marechal Rondom Avenue s/n, São Cristóvão, SE, Brazil
[b] Department of Pharmacy, Federal University of Sergipe, Marechal Rondom Avenue s/n, São Cristóvão, SE, Brazil
[c] Institute of Technology and Research, Tiradentes University, Murilo Dantas Avenue 300, Aracaju, SE, Brazil
[d] Department of Physiology, Federal University of Sergipe, Marechal Rondom Avenue s/n, São Cristóvão, SE, Brazil
[e] Post-Graduation Program in Pharmaceutical Sciences, Federal University of Rio Grande do Sul, Ipiranga Avenue 2752, Porto Alegre, 90610-000, RS, Brazil

ARTICLE INFO

Article history:
Received 17 May 2016
Received in revised form 29 August 2016
Accepted 10 September 2016
Available online 12 September 2016

Keywords:
Burn
Porcine
Gelatin membrane
Liposomes
Usnic acid

ABSTRACT

There are a range of products available which claim to accelerate the healing of burns; these include topical agents, interactive dressings and biomembranes. The aim of this study was to assess the effect of a gelatin-based membrane containing usnic acid/liposomes on the healing of burns in comparison to silver sulfadiazine ointment and duoDerme® dressing, as well as examining its quantification by high performance liquid chromatography. The quantification of the usnic acid/liposomes was examined using high performance liquid chromatography (HPLC) by performing separate in vitro studies of the efficiency of the biomembranes in terms of encapsulation, drug release and transdermal absorption. Then, second-degree 5 cm^2 burn wounds were created on the dorsum of nine male pigs, assigned into three groups (n = 3): SDZ – animals treated with silver sulfadiazine ointment; GDU – animals treated with duoDerme®; UAL – animals treated with a gelatin-based membrane containing usnic acid/liposomes. These groups were treated for 8, 18 and 30 days. In the average rate of contraction, there was no difference among the groups ($p > 0.05$). The results of the quantification showed that biomembranes containing usnic acid/liposomes were controlled released systems capable of transdermal absorption by skin layers. A macroscopic assay did not observe any clinical signs of secondary infections. Microscopy after 8 days showed hydropic degeneration of the epithelium, with intense neutrophilic infiltration in all three groups. At 18 days, although epidermal neo-formation was only partial in all three groups, it was most incipient in the SDZ group. Granulation tissue was more exuberant and cellularized in the UAL and GDU groups. At 30 days, observed restricted granulation tissue in the region below the epithelium in the GDU and UAL groups was observed. In the analysis of collagen though picrosirius, the UAL group showed greater collagen density. Therefore, the UAL group displayed development and maturation of granulation tissue and scar repair that was comparable to that produced by duoDerme®, and better than that produced by treatment with sulfadiazine silver ointment In addition, the UAL group showed increased collagen deposition compared to the other two groups.

1. Introduction

Damaged tissue provides a potent culture medium for the growth of bacteria because of its temperature and moist, nutrient rich environment (Miyazaki et al., 2012; Muzzarelli, 2009). A factor of great importance for the successful treatment of lesions is their

* Corresponding author.
E-mail address: paulanunes_se@yahoo.com.br (P.S. Nunes).

http://dx.doi.org/10.1016/j.ijpharm.2016.09.040
0378-5173/

protection from the external environment with occlusive dressings. Collagen membranes have a great advantage in this area, especially in the treatment of burns, as their characteristic resorbability means no second surgical intervention is required for their removal, avoiding postoperative complications and patient discomfort (Boateng et al., 2008; Neel et al., 2012). However, collagen membranes, which have been in use since the late 19th century, can have poor mechanical strength, shape stability and low elasticity. Gelatin-based membranes, which have been employed in recent years, are a potentially useful biomaterial without some of the problems of collagen and are especially effective in the promotion and acceleration of granulation and epithelialization (Albuquerque-Júnior et al., 2009; Dantas et al., 2011) and also allow gradual drug release within target tissues (Dias et al., 2011). Gelatin membranes containing compounds that promote wound healing can be produced. A promising compound is usnic acid, one of the best studied of the various lichen compounds (Ahmadjian, 1993). It comes from the secondary metabolism of lichens (an association between fungi and algae) and has proven healing (Nunes et al., 2011), antimicrobial (Segatore et al., 2012) and antibiotic (Honda et al., 2010) effects. However, exploiting these therapeutic qualities is difficult because the metabolic lichens have unfavorable physico-chemical characteristics, such as low water solubility. One way to overcome this is to use liposome-loaded usnic acid (UALs) combined with the gelatin membrane. Liposomes are artificially prepared membranous vesicles composed of natural phospholipids and cholesterol. Their structure is similar to the cell membrane in terms of hydrophilicity and lipophilicity, and are suitable for use as the carrier of drugs insoluble in water, such as usnic acid. It can be used to target the slow release of the drug, thereby reducing toxicity, and improving bioavailability. Liposomes are biodegradable, biocompatible, non-immunogenic and are therefore attracting increasing attention in medicine (Fan et al., 2013; Huanga et al., 2014). Previously, our group, Nunes et al. (2011), published a study of the effect of a collagen-based membrane containing usnic acid/liposome on the treatment of burns in rodents, and now, in this study, aim to evaluate the effect of a gelatin-based membrane containing usnic acid-loaded liposome in pigs, comparing two reference products used in burn treatment, silver sulfadiazine and DuoDerme®.

2. Materials and methods

2.1. Membrane preparation

The gelatin solution containing the liposomes/usnic acid was prepared using the "casting" method, in two steps. First a powdered gelatin solution containing acetic acid and a plasticizer (propylene glycol) was created and mechanically stirred for 24 h. At the same time, a lipid solution (phosphatidylcholine – Lipoid GMBH 75%) containing UA and an organic solvent (chloroform) was prepared and, through the solvent evaporation method using a rotary evaporator (24 h), a dry film was formed on the evaporator balloon. This was then resuspended in distilled water and the film detached from the balloon using mechanical agitation. Ultra sound is then used to make this into a solution. The two solutions were then mixed for 24 h using magnetic agitation, and finally for 30 min using ultra sound. This mixture was poured into glass plates and after evaporation of water a dry membrane was formed on the plate, which was cut into squares (5/5 cm) for use with the bioassay animals. Nunes et al. (2010) described the characterization of membranes.

2.2. HPLC analysis and method validation

The usnic acid was determined using an HPLC system that consisted of a degasser DGU-20A3, two LC-20AD pumps, a SIL-20A HT auto injector, a CTO-20A column oven, an SPDM20Avp photodiode array detector (DAD) and a CBM-20A system controller (Shimadzu Co., Kyoto, Japan). The analysis was performed using a Phenomenex Luna C18 analytical column of 150 × 4.6 mm (5 μm particle size). The mobile phase used was methanol–water: acetic acid 1% (90–10) with a flow rate of 1.0 mL min^{-1} and the injection volume was 20 μL. The detector was set at 280 nm for acquiring the chromatogram. The data were obtained using Shimadzu LC Solution software. The HPLC method was validated in respect of linearity, limit of detection (LOD), limit of quantification (LOQ), precision, accuracy and robustness through procedures established by the International Conference on Harmonization guidelines (ICH, 2005). The linearity was obtained using a calibration curve at five different concentrations: 5, 10, 25, 50 and 100 μg mL^{-1}. The LOD and LOQ were calculated based on the standard deviation of the y intercept (σ) and the slope of the standard calibration curve (S). LOD was calculated by the equation 3.3 σ/S and the LOQ also examined by the equation 10 σ/S. The precision of the method was investigated in relation to repeatability (intraday precision) and intermediate precision (interday precision). Six samples of usnic acid (100 μg mL^{-1}) were injected on the same day to evaluate repeatability. The intermediate precision was evaluated by analyzing usnic acid samples in the same concentration on different days and by a different analyst. The precision was expressed as relative standard deviation (RSD%). Accuracy was evaluated by using solutions containing three known concentrations (5, 50 and 100 μg mL^{-1}) of usnic acid analyzed in triplicate. Accuracy was calculated as percent recoveries of response factor (area/concentration). The ruggedness of the method was evaluated by changing the mobile phase flow rate and using different analytical columns.

2.3. Encapsulation efficiency of membranes (EE%)

The EE% was determined by dissolving a membrane segment with an area of 7 cm^2 in 10 mL of methanol under constant stirring (250 rpm) for 12 h to allow all entrapped usnic acid to be in solution. After this procedure, the solution was filtered through a 0.22 μm membrane filter and analyzed by HPLC. The samples were prepared through three different membranes and analyzed in triplicate. The EE% was calculated according to the equation:

$$EE\% = \frac{C1}{C2} \times 100 \quad (1)$$

where, C1 is the content of usnic acid present in the membrane and C2 is the usnic acid amount initially used to prepare the membrane.

2.4. In vitro *membrane release*

The usnic acid membrane release was performed with a vertical automated Franz diffusion cell (MicroettePlus Multi-Group®, Hanson Research Corporation, Chatsworth, CA, USA) operating at 32 ± 0.5 °C. The diffusion area was 1.76 cm^2 and the receptor chamber volume was 7.0 mL. A dialysis membrane (MWCO = 12 kDa, Sigma-Aldrich), pre-hydrated for 8 h was fixed between the donor and the receptor compartments. Sink conditions were maintained using a receptor medium composed of 2% (v/v) DMSO. Sample aliquots (2 mL) were collected each 0, 0.25, 0.5, 1, 2, 4, 6, 8, 10, 12, 18 and 24 h and analyzed by HPLC.

2.5. Transdermal absorption of usnic acid from the membranes

The transdermal absorption studies were conducted using porcine ear skin as the membrane. The membrane samples were donated from a regional slaughterhouse (Bento Gonçalves, Brazil).

Excess fat tissue, hypodermis and hair were removed, maintaining the full-thickness of the skin. The surface was cleaned with water before storage at −20 °C in aluminum foil until use. Before each experiment, the skin was cut into round slices, and all skin slices used had a width of between 1.8 and 2.2 mm measured with a dial thickness gauge (No. 7301®, Mitutoyo, Japan). The skin permeation study was performed using an automated Franz cell (MicroettePlus Multi-Group®, Hanson Research Corporation, Chatsworth, CA, USA), for 24 h. The receptor medium used to the guarantee skin condition was 7 mL of 2% (v/v) DMSO aqueous solution. The membrane was manually applied on the diffusion area (1.76 cm^2) with saline. The cells were occluded with a glass cover. The acceptor phase was maintained under constant stirring at 32 °C during the entire experiment. Samples of 2 mL were withdrawn from the acceptor phase automatically into vials at determined intervals up to 24 h, and these were injected into the HPLC system. The collected aliquots were replaced with fresh solution. The stratum corneum was removed by the tape stripping technique, before assay for 1 st degree simulated injury, using 18 tape stripes (3M® Brasil; Sumaré, Brazil). At the end of 24 h, the epidermis and dermis were separated using a warm (60 °C) water bath for 45 s followed by removal with a scalpel. Usnic acid was extracted with methanol from all layers of the skin: epidermis (3 mL) and dermis (3 mL). The extraction was performed by 2 min of vortex followed by 30 min of sonication. The samples were filtered into vials before HPLC analysis (Serafini et al., 2014).

2.6. Animal management and ethics

Three burn lesions were created in the dorsum of nine large-white *Yorkshire* male pigs (25–30 kg, from the same litter, approximately 90 days old). A physical and hematological examination, as well as a parasitological analysis (Willis method), was performed on the animals in order to ensure they were healthy and eligible for the study. The animals received water and swine diet (Purina Nutrimentos LTDA – Ribeirão Preto – SP) and were housed in individual 3 m^2 cages in the vivarium of the Federal University of Sergipe. All the experiment was supervised by a veterinarian. Experimental protocols and procedures were approved by the Animal Care and Use Committee of the Federal University of Sergipe (CEPA/UFS # 69/2010).

2.7. Burning procedures

The burn lesions were carried out under sedation with intramuscular administration of chlorpromazine (3 mg/kg). Intravenous administration of ketamine hydrochloride (2 mg/kg) and midazolam (0.08 mg/kg) were subsequently carried out for general anesthesia using a catheter (20G) in the marginal ear vein. Two additional doses of intravenous anesthesia (half of the induction dose) were given for the maintenance of anesthesia. Lesions were quadrangular (25 cm^2), 4 cm from the spinal column and 4 cm from each other (Papp and Valtonen, 2006). A bronze tool, coupled with a thermometer, was heated in the blue flame of a Bunsen burner to 90 °C. The tool was pressed on the animal's skin for 20 s in order to create the burn lesions (Temperature settings and plate contact time on the skin were established in a pilot study) (partial – Hunt et al., 1998).

The lesions were then randomly treated with silver sulfadiazine ointment (SDZ), DuoDerme® wound dressing (GDU) or gelatin-based membrane containing usnic acid-loaded liposome (UAL) and dressed with a cotton gauze and a protective covering (Fig. 1). At the end of the experimental procedures, Ibuprofen (4 mg/kg) and penicillin (20,000 IU/kg) were administered (via the intramuscular route) in all the animals. At 8, 18 and 30 days after the burn procedures, three animals were euthanized and the wounded skin areas were surgically removed for further histological examination.

2.8. Gross evaluation

Prior to the euthanization of the animals, a descriptive gross evaluation of the wounded skin areas was performed examining to the following features: necrosis, suppuration, granulation tissue formation and wound retraction. Furthermore, the burns were measured (length × width) using digital pachymetry (digital caliper Digimess®) to assess the size of the wound. During the experiment, the burn lesions were exposed to reapply the

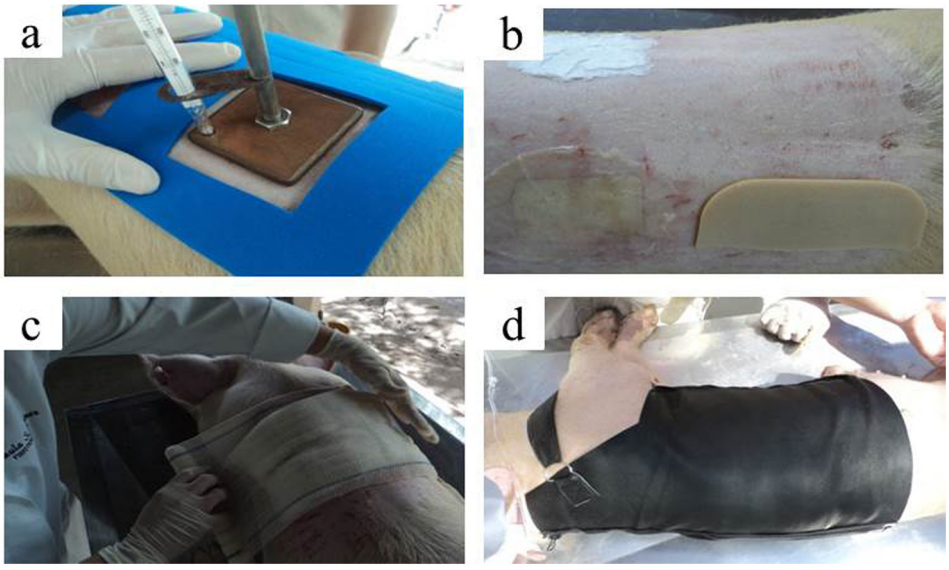

Fig. 1. Phases of the methodological procedures: (a) burn induction procedure; (b) covering of the lesions with the products; (c) covering of the lesion with cotton gauze; (d) covering of the lesions with protective dressing.
Source: AUTHOR

medicines every four days. Subsequently, the animals were euthanized through the administration of chlorpromazine (3 mg/kg) and sodium thiopental (40 mg/kg), and the wound areas surgically removed and formalin-fixed for further histological examination.

2.9. Histological procedures

The sample was hemi-sectioned and each section was fragmented into four horizontal sections (fragments A, B, C and D). These fragments were then again sectioned into four gross sections, so that each sample (hemi-section) was represented by 16 gross sections. All the specimens were dehydrated, diaphonized and embedded in paraffin according to routine laboratorial techniques. Sixteen serial 5 μm thick histological slides were produced from each paraffin-embedded sample, and stained in hematoxylin-eosin and picrosirius.

2.9.1. Assessment of the histological burn healing grading

A detailed descriptive analysis of the histological features of the epithelial lining, inflammatory response, granulation tissue and fibrous scar formation in each group was performed, and the burn healing progress was scored as described in Table 1. The mean scores were obtained by calculating the ratio between the sum of the scores of each histological section and the number of sections analyzed per group.

2.9.2. Assessment of collagen deposition

Histological sections stained in Sirius Red and analyzed under polarized light were used to perform the descriptive analysis of the collagenization. Collagen fibers were analyzed according to their birefringence pattern (greenish/yellow-greenish or orange, orange-reddish), morphological appearance (wavy or stretched, thin or thick, short or long), and architectural arrangement (reticular, parallel or interlaced).

2.10. Statistical analysis

The size of the wound area was subjected to the Shapiro Wilk test to assess the normality of the data, and then the means were compared between the groups at the different times using Analysis of Variance (ANOVA) and Tukey's test. The mean scores of the histological burn healing grading were analyzed with the Kruscall Wallis test, followed by Dunn's test. The average values obtained from the quantitative analysis were compared using a confidence level of 95% ($p < 0.05$).

3. Results

3.1. HPLC analysis and encapsulation efficiency (EE%)

The usnic acid peak obtained excellent chromatographic resolution in the 280 nm wavelength with a retention time of 7 min. The method showed good linearity in the concentration range of 5–100 $\mu g\,mL^{-1}$, obtaining a regression equation of $y = 92376x + 42438$ and $R^2 = 0.9998$. The LOD and LOQ were 0.28 and 0.83 $\mu g\,mL^{-1}$, respectively. The repeatability tests showed 0.12% RSD, and intermediate precision tests showed 0.79% RSD (day 1) and 0.41% RSD (day 2). These values can be considered excellent for analytical procedures as they showed RSD of less than 1%. The mean percent accuracy values and RSD% for analyzes in low (5 $\mu g\,mL^{-1}$), medium (50 $\mu g\,mL^{-1}$) and high (100 $\mu g\,mL^{-1}$) concentrations were 100.4%, 0.66%; 100.1%, 0.30%; 99.8%, 0.49%; respectively. The accuracy results were satisfactory, obtaining RSD of less than 5%. The robustness was evaluated changing the flow rate (0.8, 1.0, 1.2 $mL\,min^{-1}$) and using different columns (C18 250 × 4.6 mm and C18 150 × 4.6 mm). The method was found to be robust as there were no significant modifications in the chromatograms.

The EE% is a quantitative parameter that was utilized to calculate the amount of usnic acid entrapped in the membrane. The EE% were calculated using Eq. (1) and the usnic acid amount initially used to prepare the membrane was 183.54 μg in a membrane segment with 7 cm^2 area. The content of usnic acid present in the membrane after HPLC analysis was 172.07 ± 0.27 μg with an EE% of 93.75%. The EE% value was close to 100% indicating that almost all the usnic acid was encapsulated in the membrane.

3.2. In vitro *release of usnic acid from the membrane*

Fig. 2a shows the *in vitro* release profile of usnic acid from the membrane. The curve was obtained based on the percentage of usnic acid released as a function of time. The initial burst phase occurred until 4 h after the start of the experiment, releasing 38.70% (16.31 $\mu g\,cm^{-2}$) of the usnic acid present in the membrane, characterizing fast drug release. However, after 4 h and until 24 h after the start of the experiment, the UAL showed a controlled pattern reaching 98.15% (41.37 $\mu g\,cm^{-2}$) of usnic acid released.

3.3. Transdermal absorption of usnic acid from the membrane

The transdermal absorption studies of usnic acid from the UAL were performed by comparing the detected amounts of usnic acid ($\mu g\,cm^{-2}$) in different skin layers (epidermis, dermis) and in the receptor fluid. The profile is presented in Fig. 2b. The amount of usnic acid in the epidermis was 3.54 ± 0.79 $\mu g\,cm^{-2}$. However, a larger amount of usnic acid was quantified in the dermis (13.64 ± 0.17 $\mu g\,cm^{-2}$). This result shows a significant difference ($p < 0.0001$) for the amount of usnic acid in the skin layers because the active compound tended to accumulate in the dermis in larger amounts, when compared with the epidermis, and was probably able to be systemically absorbed. The determination of the receptor fluid, which is considered the permeated amount in the systemic circulation, was quantified after 24 h and was 4.1 ± 0.32 $\mu g\,cm^{-2}$. These results corroborate those observed in

Table 1
Scores for the histological characterization of the granulation tissue.

Score	Characterization of the granulation tissue
0	Absence of granulation tissue
1	Granulation tissue little evident and immature, composed predominantly by malformed vessels (in gaps) and endothelial cells disposed in a disorganized way.
2	Granulation tissue stretching up to 1/3 above the hypodermis, composed predominantly of malformed vessels (in gaps) and endothelial cells disposed in a disorganized way.
3	Granulation tissue occupying more than 1/3 of the dermis, composed predominantly by malformed vessels (in gaps) and endothelial cells disposed in a disorganized way.
4	Granulation tissue limited to the upper 2/3 of the dermis, composed predominantly of fibroblasts and collagen fibers.
5	Complete replacement of the granulation tissue through primary fibrous scarring.

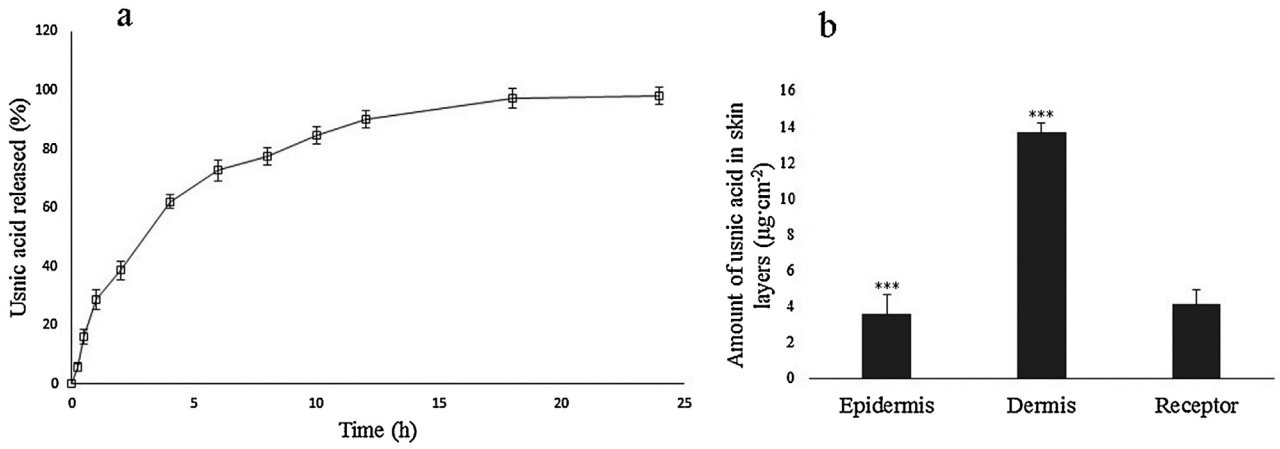

Fig. 2. (a)In vitro release profile of usnic acid membranes in DMSO 2% receptor medium (n = 6). (b) Skin penetration and permeation profile of usnic acid in DMSO 2% receptor medium. *** ($p < 0.0001$).

the release experiment that showed usnic acid controlled release over time.

3.4. Gross

3.4.1. Clinical characteristics of the burn

On day 8, the burns were square shaped, with erythematous edges and a creamy white pseudo-membranous necrotic background. On day 18, there was clear retraction of the burn wounds, associated with the development of a reddish vascular tissue, consistent with granulation tissue, observed on the surface of the injured skin in all groups. On day 30, extensive retraction of the burn wounds edges was seen in all the groups, suggesting the success of the healing process. Moreover, no clinical sign of abscess (suppurative exudate) or cellulitis (caused by purulent spreading to the muscular fascia), as well as hypertrophic or atrophic scarring, was observed in this experiment, suggesting the healing course was uneventful (Fig. 3).

3.4.2. Index analysis of the wound area by burns

The mean size of the burn wound areas reduced progressively during burn healing in all three groups (Fig. 4). The greatest reduction in rates of burn wounds occurred between days 8 and 18. However, no significant differences between the mean areas of the burn wound in a comparison among the groups were observed, regardless of the experimental time of measurement ($p > 0.05$).

3.5. Hematoxylin-eosin microscopy

3.5.1. Semi-quantitative analysis of granulation tissue (SAGT)

On day 8, no significant difference in the mean SAGT score was observed between the UAL and GDU groups ($p > 0.05$), however, the mean score obtained in UAL group was significantly higher than in the SDZ group ($p = 0.016$) at this time. Moreover, no difference was observed on day 18 ($p = 0.6101$) or day 30 ($p = 0.7550$) between the groups (Fig. 5).

3.5.2. Analysis of re-epithelialization, inflammatory reaction and granulation tissue

On day eight, an acute inflammatory response was observed underneath irregular strands of necrotic fibrous tissue on the surface of the burn wounds, but the neutrophils content was massive in the UAL group (Fig. 6c) and moderate in the GDU and SDZ groups (Fig. 6b and a). The formation of granulation tissue was limited to the hypodermis in the SDZ group (Fig. 6a), but extended to the reticular dermis in the GDU and UAL groups (Fig. 6b and c). Squamous epithelial lining was restricted to the histological edges of the burn wounds, and presented extensive hydropic degeneration and neutrophilic exocytosis in SDZ group.

On day 18, all three groups showed intense granulation tissue extending from the surface to the bottom of the burn wounds. Despite the high content of neoformed blood vessels, the fibroblastic component of the granulation tissue was markedly more evident in the GDU and UAL groups (Fig. 6e and f) than in SDZ group (Fig. 6d). The inflammatory response observed in the SDZ group remained remarkable (Fig. 6e) in contrast to the moderate infiltrate limited to the center and surface of the wounds seen in the other groups. A hyperplastic squamous epithelial lining covering approximately 10–30% of the burn wound surface was observed in the GDU and UAL groups, whereas less than 10% was covered in the SDZ group. Additionally, a thin but well-developed granular layer was seen in some areas of the epithelial lining of the UAL and GDU groups.

On day 30, the granulation tissue in GDU and UAL groups (Fig. 6h and i) was limited to the upper third of the dermis, and was shown to be rich in fibroblast-like spindle-shaped cells with mild residual lymphocytic inflammatory response. In the SDZ group, the granulation tissue still presented a bottom-to-top distribution throughout the healing area, with moderate infiltration of mononuclear inflammatory cells (Fig. 6g1 and g2). Furthermore, the GDU and UAL groups showed full recovery of the burn wound surfaces (Fig. 6h and i), whereas in the SDZ group although the epithelial lining covered more than 80% of the wounds (Fig. 6g1 and g2), full epithelization was not seen in this group.

3.6. Sirius red microscopy

On day 8, the three groups exhibited a similar morphological pattern, characterized by short thick gross fibers, with yellow birefringence. The interfibrillar spaces were rather irregular (Fig. 7a–c). On day 18, the SDZ and GDU groups presented short, thin, delicate collagen fibrils, with green birefringence on the top of the burn wounds, but yellow on the bottom. The fibrils were set in a reticular arrangement and the interfibrillar spaces were large and abundant (Fig. 7d and e). The UAL group presented longer fibrils and fibers, with strong yellow/orange birefringence, in a reticular arrangement on the top of the burn wounds, but parallel-arranged on the bottom. The fibrils and fibers were densely deposited throughout the healing area, with smaller and less apparent interfibrillar spaces (Fig. 7f). On day 30, all the groups showed the presence of collagen fibers with yellow birefringence. The SDZ group presented lower collagen condensation than the other two

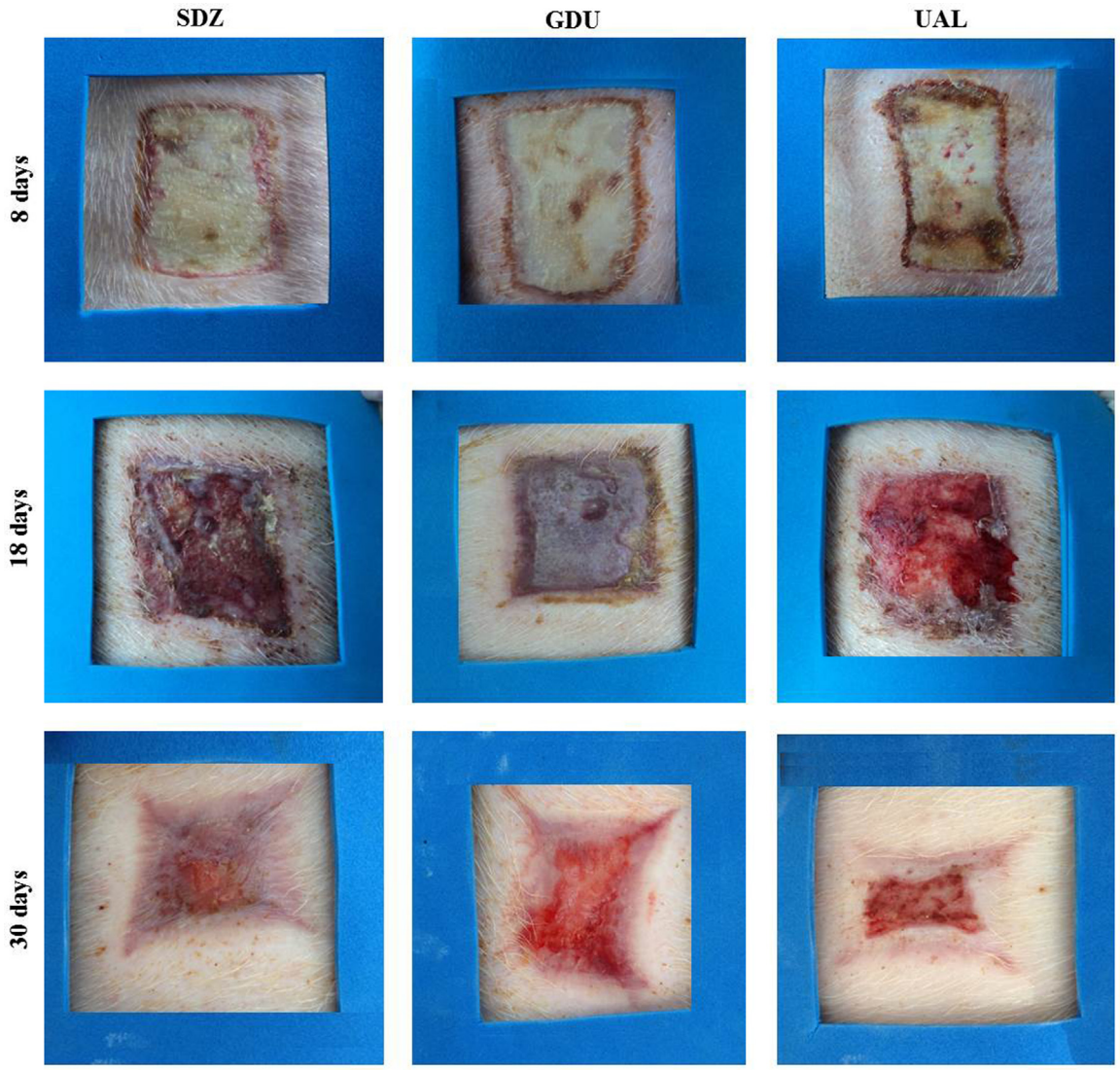

Fig. 3. Macroscopy of the wounds treated with silver sulfadiazine (SDZ); DuoDerme® (GDU) and gelatin membrane with usnic acid/liposomes (UAL) at 8, 18 and 30 days. Source: AUTHOR

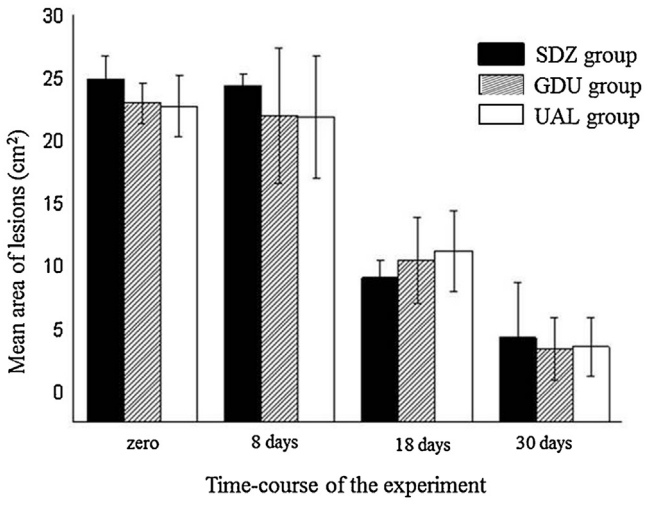

Fig. 4. Mean index of the wound areas by burn, at the initial time (burning induction) and 8, 18 and 30 days after the lesion, in the three experimental groups.

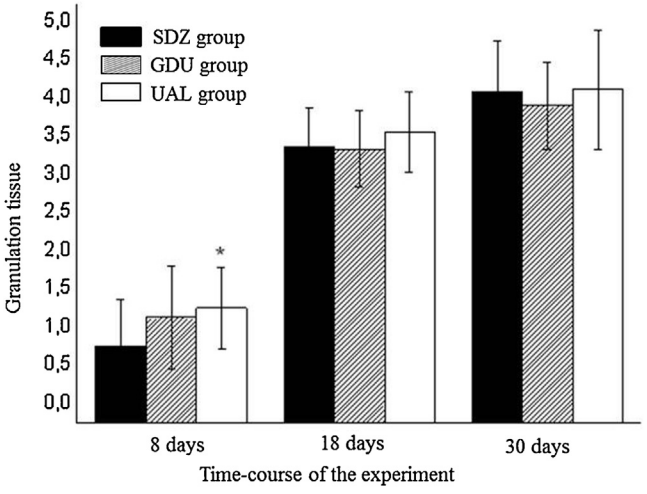

Fig. 5. Semi-quantitative analysis of the evolving profile of the granulation reaction throughout the experimental time in the SDZ, GDU and UAL groups. (*) significant difference between the UAL and SDZ groups at 8 days.

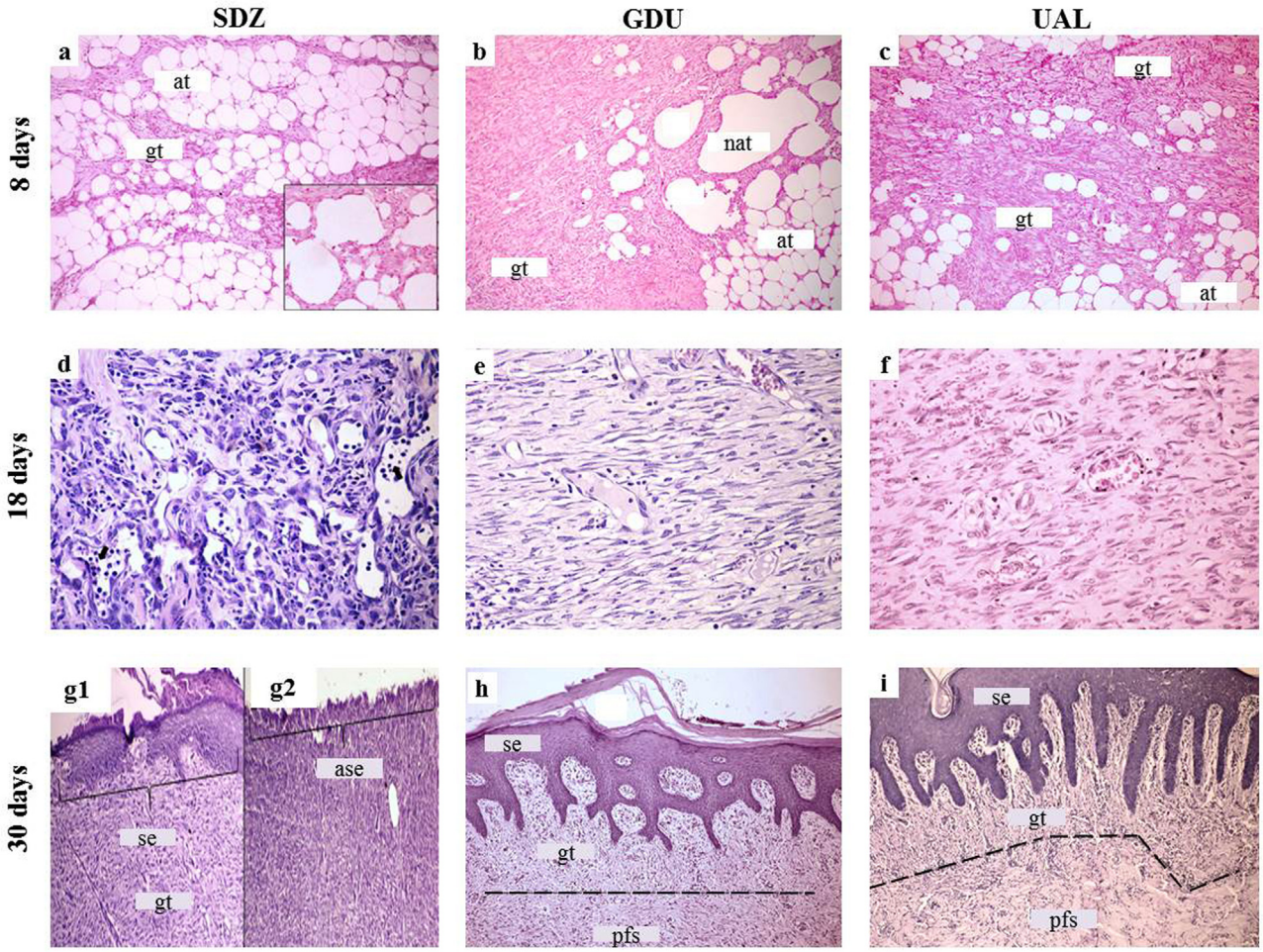

Fig. 6. Hematoxylin-eosin microscopy of the SDZ, GDU and UAL groups at 8, 18 and 30 days after the dermic burn lesion. (a) immature granulation tissue (gt) within the hypodermic fatty tissue (at) (100×). Highlighted, the irregular and anuclear necrotic fatty tissue (400×); (b) Granulation tissue (gt) permeating the necrotic fatty tissue (nat); (c) Immature granulation tissue (gt) and inflammatory infiltration on the reticular dermis (lt) (100×); (d) Fibrovascular granulation tissue permeated by inflammatory infiltrate on the surface; (e) Granulation tissue showing a great number of irregular blood vessels (400×); (f) Granulation tissue with cellularization and vascularization in the depth of the specimen (400×); (g1) area showing scaly epithelial covering (se); (g2) area showing lack of scaly epithelial (ase) (100×); (h) and (i) surface completely covered by scaly epithelial (se). On the surface dermis residual granulation tissue (gt) and in the deeper portion, the primary fibrous scar (pfs) (100 x); (i) Hyperplasic scaly epithelium (se) covering all the scarring area. Underlying, demarcation between the narrow area of the residual granulation tissue (tg) and the deep fibrous scar (pfs) composed of thick fibers densely compacted by collagen (100×).

groups. The fibers were predominantly thin, with variable length, arranged in a disorganized pattern, with large interfibrillar spaces (Fig. 7g). The GDU group showed dense deposition of parallel-arranged short, thin fibers, with narrowed interfibrillar spaces (Fig. 7h). The UAL group presented extensive condensation of grosser and thicker collagen fibers, throughout the extent of the healing area. The interfibrillar spaces were narrowed and less apparent than in the other groups (Fig. 7i).

4. Discussion

In this study, usnic acid was used to improve burn healing. As usnic acid is insoluble in water, the drug was loaded within liposomes, since the structure of these phospholipid vesicles, with hydrophilicity and lipophilicity, is suitable to use as a carrier of poorly-water soluble substances (Fan et al., 2013). Liposomal vesicles also provide slow release, reducing toxicity and improving the bioavailability of the drug (Huanga et al., 2014). Gelatin-based matrices were used in this study as dressing membranes to carry (+)-usnic acid-loaded liposomes. Thus, these liposome-gelatin membranes worked as simple technological systems to provide controlled delivery of the drug into the burn site.

Examination of the resulting drug release by HPLC confirmed that UAL was capable of controlling the release of usnic acid. Yang et al. (2015) in a previous study conducted with vancomycin hydrochloride liposomes, reported a similar release profile as the present study, with a burst phase at 4 h and 94% of drug release by 10 h. The controlled release can be explained because the lipid shell of the liposomes entrap the drug, releasing it gradually from the lipid matrices. Thus, the membranes containing usnic acid/liposome could maintain a constant drug concentration for a prolonged time, providing an opportunity to reduce the frequency of administration.

Indeed, because of the way that the drug is released, it penetrates and permeates the layers of skin, showing the drug delivery system's characteristic transdermal capabilities. In a study by Serafini et al. (2014), a formulation containing free usnic acid incorporated in hydroxyethyl cellulose-gel demonstrated its potential for transdermal application, a finding corroborated by our study, and was shown to be capable of penetrating the stratum corneum, the main barrier to a substance permeating the skin and the most significant rate limiting factor (Prow et al., 2011). In our study, the stratum corneum was removed to simulate 1st degree injury to evaluate the penetration/permeation profile in lesioned

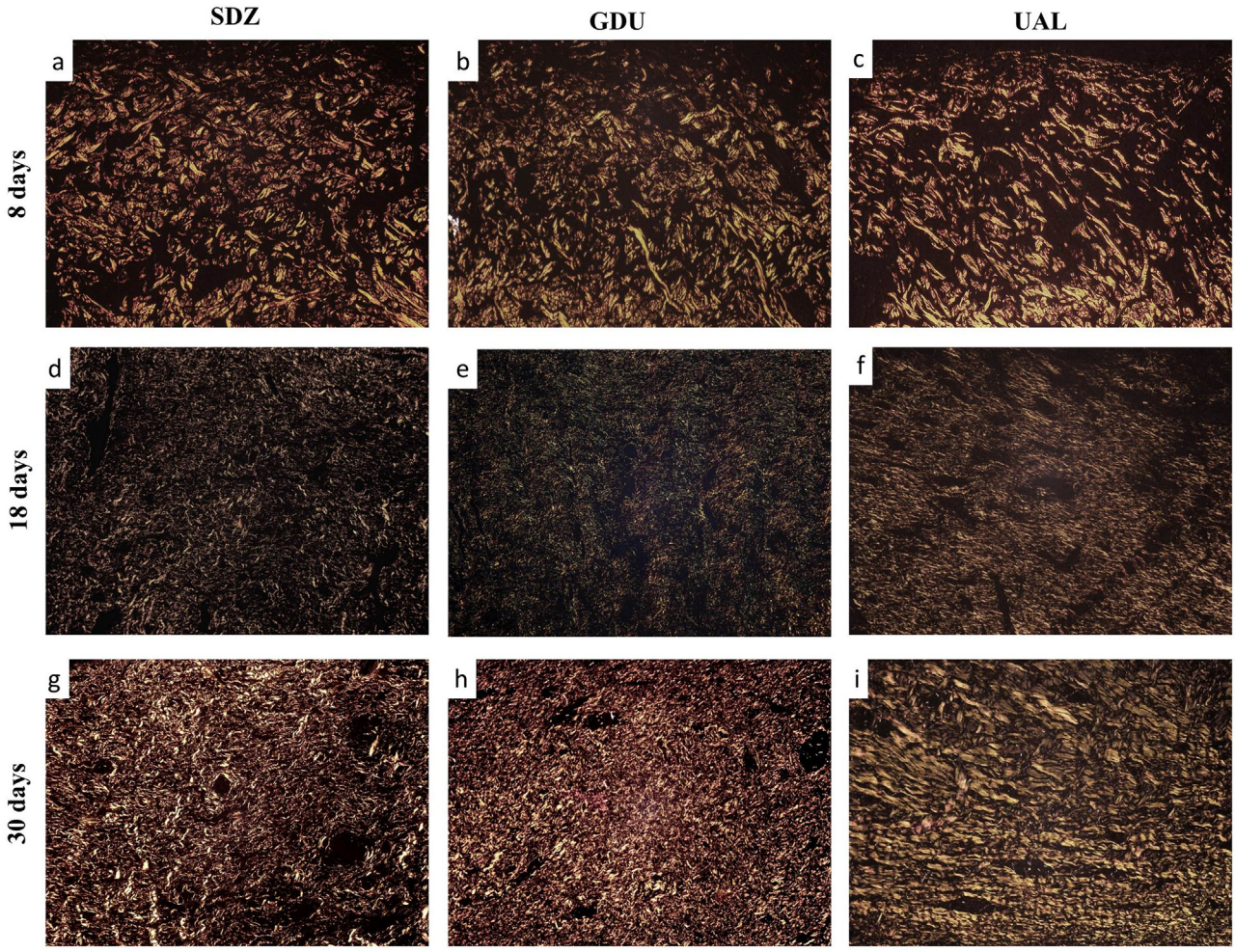

Fig. 7. Sirius red microscopy in the SDZ, GDU and UAL groups at 8, 18 and 30 days after the dermic lesion burn. Characteristics of the fibrils and/or collagen fibers; and characteristics of the interfibrillar spaces.

skin. Some studies have also reported that liposomes, in comparison with other drug delivery systems, offered higher skin retention due to the presence of phospholipids in their biocompatible constructs (Clares et al., 2014; Raza et al., 2013). Hence, usnic acid is a promising molecule for use in a transdermal formulation because of its high retention and ability to penetrate and permeate the stratum corneum and reach the blood circulation.

In the three groups at eight days, there was coagulative necrosis of the conjunctive tissue and intense acute inflammatory reaction, typical of the morphological characteristics of this phase of scar repair (Samy et al., 2012; Velnar et al., 2009). Another observation at this experimental time was that the granulation reaction observed in the central region of the wounds of the SDZ group was restricted to the adipose panicle and was more immature than in the GDU and UAL groups. This was possibly due to the occlusion generated by duoDerme® and the gelatin membrane, which led to increased protection of the wound surface against microorganisms. In addition, gelatin membranes have been regarded as excellent biomaterials for wound dressing because they favor the adherence and migration of fibroblasts throughout the film matrix (Yeh et al., 2011) and present high hygroscopicity, biodegradability and biocompatibility (Wanga et al., 2012).

The role played by usnic acid on the pathophysiological events associated with the development of granulation tissue, such as the proliferation of fibroblasts and endothelial cells and myofibroblast differentiation, is not fully clarified. As usnic acid does not seem to directly affect the fibroblasts and endothelial cell proliferation and function, it is possible that the biological activities induced by this molecule result from indirect effects. It has been demonstrated that usnic acid inhibits the secretion of pro-inflammatory cytokines and mediators, such as tumor necrosis factor-alpha (TNF-α), interleukin-6 (IL-6), interleukin-1 beta (IL-1β), induced nitric oxide (iNOS) and cyclooxygenase-2 (COX-2), and also increases the release of the anti-inflammatory molecules IL-10 and HO-1 in a dose-dependent relation (Huanga et al., 2014).

Furthermore, usnic acid showed antibacterial activity against *Enterococcus faecium, faecalis* and *Staphylococcus aureus* (Elo et al., 2007). Bacteria commonly associated with burn wound infections (Alebachew et al., 2012; Church et al., 2006). Therefore, the reduction of the inflammation magnitude and bacterial load could favor a faster chronification of inflammation and consequent earlier formation of granulation tissue.

At 18 days, the epidermal neoformation, although partial in the three groups, was shown to be quite incipient in the SDZ group compared to the GDU and UAL groups. Thus, it can be suggested that both membranes used in this study have fostered a more humid environment at the wound bed, promoting neogenesis of the epidermis, while the ointment formulation of sulfadiazine may have suffered premature drying and did not prevent the

evaporation of water from the wound. Some authors have shown that synthetic or natural polymers, when used in dermal scarring, are able to prevent dehydration of the wound (Chen et al., 2013; Jayakumar et al., 2011). Neel et al. (2012) assert that a moist environment promotes the migration of epithelial cells, which promotes an occlusive barrier against the external environment. It is worth noting that the moisture from the wound bed can facilitate the arrival of keratinocytes to the injury. Thescher et al. (2013) demonstrated that polymeric structures can interfere positively in the relative density and viability of keratinocytes and fibroblasts in the wound.

The wound healing ability of usnic acid derivatives has been tested on an *in vitro* wound healing model consisting of monolayers of HaCaT keratinocytes by Michela et al. (2013). They noted that the usnic acid (GABA–usnic acid derivative 9) induced the highest wound closure rate, almost approaching the wound healing potential of the platelet lysate, a blood derivative used as reference substance. Linear incision by using a tensiometer and circular excision wound models were also employed *in vivo* in this study. In the linear incision wound model, usnic acid was shown to be highly effective when compared to the negative control (statistically-significant) and the gold standard (not statistically-significant). In relation to the contraction of the progression healing of wounds on a circular excision wound model, the usnic acid (components 9, 7 and 8) had a higher percentage of contraction (statistically significant) when compared to the negative control. The usnic acid (component 9) showed no significant difference when compared to the gold standard (Michela et al., 2013).

Another important finding was the reaction of granulation, which was more immature in the SDZ group, than in the GDU and UAL groups. The acceleration in the granulation dynamics in the GDU and UAL groups compared to the SDZ group probably occurred as a result of the frame structure formed by the gelatin that both materials contain. Yeh et al. (2011) reported that the reticulated gelatin, as conveyed in the form of membranes, provides greater adherence and migration of fibroblasts throughout the film matrix. Furthermore, the epidermal neo-formation 30 days after the burns were significantly less expressive in the SDZ group compared to the two other groups. These findings suggest that, as reported by Neel et al. (2012) and Thescher et al. (2013) synthetic materials increase the viability of keratinocytes in the wound.

Burlando et al. (2009) studied five compounds representative of major structural classes of lichen polyketides, including usnic acid. They were investigated for their ability to affect cell proliferation or wound healing, two functional targets of relevance for research on cancer or tissue regeneration. The experiments were carried out on MM98 malignant mesothelioma cells, A431 vulvar carcinoma cells, and HaCaT keratinocytes. They noted that usnic acid was the lichen component that most induced wound closure and one of those which most stimulated cell migration.

Possibly, the mechanism of action is through its large capacity to affect cell proliferation or to promote motility and wound healing, thus suggesting that wound healing resulted from stimulation of motility rather than from mitosis. At the end of the experiment, in the SDZ group, the presence of inflammatory infiltrate involved in the granulation reaction was still observed, suggesting therefore that wounds treated with the membranes in the GDU and UAL groups were in a more advanced healing phase. These findings corroborate previous reports by Mohajeri et al. (2011), who stated that silver sulfadiazine does not seem to have any direct effect on the inflammatory response during wound healing. However, current studies show the protective effect of usnic acid on Lipopolysaccharide induced (LPS) acute lung injury (ALI) in mice. In this study, usnic acid attenuated the expression of TNF-α, IL-6, IL-8 and macrophage inflammatory protein-2 (MIP-2). Meanwhile, an improved level of IL-10 was observed (Su et al., 2014). These results may suggest that the reduction in intensity of the inflammation leads to greater control of the inflammatory phase of wound healing and consequently the advance of the subsequent stages. The proliferative phase would start sooner, with the development of the granulation reaction promoting accelerated healing dynamics for complete wound closure, confirming results found in the semi-quantitative analysis of the reaction of granulation by hematoxylin eosin (HE) in 8 days, and the dynamics of collagen deposition in the final stages of the process of scar repair by picrosirius in this study.

In the early stages of the repair, type-I thick, coarse and interwoven collagen with more delicate and irregular fibrils were observed in all groups. However, these fibers represent a possible persistence of the necrotic fibrous tissue. It is well established that the birefringence of collagen fibers occurs because of the presence of large amounts of basic amino acids that react strongly with acidic molecules that make up the dye, which are arranged parallel to the axial axis of the collagen molecules. The increase in the birefringence detected in polarized light is thus due to the increase in the number of parallel oriented molecules (Montes and Junqueira, 1991).

While the necrotic fibrous tissue does not present immediate changes in its quota of basic amino acids, one may suggest that in polarized light, it is not possible to distinguish necrotic or viable fibers tissue. Stromal cytomorphological changes evidenced in HE indicate that the fibrous tissue is, in fact, necrotic, and corroborate this theory. In addition, areas with large interfibrillar spaces and smaller collagen may represent regions with accumulation of leukocytes which have accelerated the degradation of collagen in necrotic tissue (Shvyrkov and Yanushevich, 2013).

In subsequent experimental periods, the predominant presence of type III collagen fibrillar intercalated with type I fibrils suggests that the necrotic tissue has been adequately removed and replaced with immature collagen. In the current study, the UAL group showed increased collagen deposition in relation to the SDZ and GDU groups. Previous studies using rodent models had already provided strong evidence that usnic acid mixed with film collagen matrices have positive modulatory action on the synthesis of scar collagen (Nunes et al., 2011). The predominance of type I collagen in the whole extent of lesions of the UAL group also suggests that the remodeling phase, represented by the degradation of a crude matrix composed of connective tissue, and the gradual and progressive deposition of new matrix containing type I and Type III collagen was more developed in this group (Almeida et al., 2013; Dantas et al., 2011; Nunes et al., 2011).

Michela et al. (2013) evaluated the wound healing activity of usnic acid. Treated skin samples were assessed for their hydroxyproline content, which gives an estimate of collagen concentration. Usnic acid (Compounds 7, 8 and 9) increased the hydroxyproline content when compared to the negative control (statistically significant) and had no significant difference with the gold standard.

5. Conclusion

It is possible to conclude that in the porcine model, the use of gelatin membranes containing usnic acid/liposomes promoted the healing and macroscopic shrinkage of the wound due the controlled release of drug. Like the other products tested, they also promoted the development and maturation of the granulation reaction over the scar repair, comparable in effect to duoDerme® and better than silver sulfadiazine ointment, and also promoted a greater increase in collagen deposition in the final stages of the experiment compared to the other products tested.

Conflict of interests

The authors declare that there is no conflict of interests regarding the publication of this paper.

Acknowledgments

The authors would like to thank the Conselho Nacional de Desenvolvimento Científico e Tecnológico (CNPq/Brazil) and Fundação de Amparo a Pesquisa do Estado de Sergipe (FAPITEC-SE) for the financial support.

References

Ahmadjian, V., 1993. The Lichen Symbiosis. John Wiley & Sons, Inc., New York, pp. 250.
Albuquerque-Júnior, R.L.C., Barreto, A.L.S., Pires, J.A., Reis, F.P., Lima, S.O., Ribeiro, M. A.G., Cardoso, J.C., 2009. Effect of bovine type-I collagen-based films containing red propolis on dermal wound healing in rodent model. Int. J. Morphol. 27, 1105–1110.
Alebachew, T., Yismaw, G., Derabe, A., Sisay, Z., 2012. *Staphylococcus* aureus burn wound infection among patients attending yekatit 12 hospital burn unit, addis ababa, Ethiopia. Ethiop. J. Sci. 24 (4), 209–212.
Almeida, E.B., Cardoso, J.C., Lima, A.K., Oliveira, N.L., Pontes-Filho, N.T., Lima, S.O., Souza, I.C.L., Albuquerque-Júnior, R.L.C., 2013. The incorporation of Brazilian propolis into collagen-based dressing films improves dermal burn healing. J. Ethnopharmacol. 147 (2), 419–425.
Boateng, J.S., Matthews, K.H., Stevens, H.N.E., Eccleston, G.M., 2008. Wound healing dressings and drug delivery systems: a review. J. Pharm. Sci. 97 (8), 892–923.
Burlando, B., Ranzato, E., Volante, A., Appendino, G., Pollastro, F., Verotta, F., 2009. Antiproliferative effects on tumour cells and promotion of keratinocyte wound healing by different lichen compounds. Planta Med. 75, 607–613.
Chen, Q., Lianga, S., Thouas, G.A., 2013. Elastomeric biomaterials for tissue engineering. Polym. Sci. 38, 584–671.
Church, D., Elsayed, S., Reid, O., Winston, B., Lindsay, R., 2006. Burn wound infections. Clin. Microbiol. Rev. 19 (2), 403–434.
Clares, B., Calpena, A.C., Parra, A., Abrego, G., Alvarado, H., Fangueiro, J.F., Souto, E.B., 2014. Nanoemulsions (NEs), liposomes (LPs) and solid lipid nanoparticles (SLNs) for retinyl palmitate: effect on skin permeation. Int. J. Pharm. 473, 591–598.
Dantas, M.D.M., Cavalcante, D.R.R., Araújo, F.E.N., Barreto, S.R., Aciole, G.T.S., Pinheiro, A.L.B., Ribeiro, M.A.G., Lima-Verde, I.B., Melo, C.M., Cardoso, J.C., Albuquerque-Júnior, R.L.C., 2011. Improvement of dermal burn healing by associating sodium alginate/chitosan-based films and low level laser therapy. J. Photochem. Photobiol. B 6, 1–9.
Dias, A.M.A., Braga, M.E.M., Seabra, I.J., Ferreira, P., Gil, M.H., Sousa, H.C., 2011. Development of natural based wound dressings impregnated with bioactive compounds and using supercritical carbon dioxide. Int. J. Pharm. 408, 9–19.
Elo, H., Matikainen, J., Pelttari, E., 2007. Potent activity of the lichen antibiotic (+)-usnic acid against clinical isolates of vancomycin-resistant enterococci and methicillin-resistant Staphylococcus aureus. Naturwissenschaften 94, 465–468.
Fan, Y., Liu, J., Wang, D., Song, X., Hu, Y., Zhang, C., Zhao, X., 2013. The preparation optimization and immune effect of epimedium polysaccharide-propolis flavone liposome. Carbohyd Polym. 94 (1), 24–30.
Honda, N.K., Pavan, F.R., Coelho, R.G., Andrade, L.S.R., Micheletti, A.C., Lopes, T.I.B., Misutsu, M.Y., Beatriz, A., Brum, R.L., Leite, C.Q.F., 2010. Antimycrobacterial activity of lichen substances. Phytomedicine 17, 328–332.
Huanga, Y., Wub, C., Liu, Z., Hu, Y., Shi, C., Yu, Y., Zhao, X., Cui Liu, C., Liu, J., Wu, Y., Wang, D., 2014. Optimization on preparation conditions of Rehmannia glutinosa polysaccharide liposome and its immunological activity. Carbohydr. Polym. 104, 118–126.
Hunt, J.P., Hunter, C.T., Brownstein, M.R., Giannopoulo, S.A., Hultman, C.S., Deserres, S., Bracey, L., Frelinger, J., Meyer, A.A., 1998. The effector component of the cytotoxic T-lymphocyte response has a biphasic pattern after burn injury. J. Surg. Res. 80 (2), 243–251.
ICH, International Conference on Harmonisation, Q2 (A), 2005. Validation of analytical procedures: text and methodology. International Conference on Harmonization. ICH, International Conference on Harmonisation, Geneva, pp. 1–13.
Jayakumar, R., Prabaharan, M., Kumar, P.T.S., Nair, S.V., Tamura, H., 2011. Biomaterials based on chitin and chitosan in wound dressing applications. Biotechnol. Adv. 29, 322–337.
Michela, B., Trucchi, B., Burlando, B., Ranzato, E., Martinotti, S., Akkol, E.K., Suntar, I., Keles, H., Verotta, L., 2013. (+)-Usnic acid enamines with remarkable cicatrizing properties. Bioorg. Med. Chem. 21, 1834–1843.
Miyazaki, H., Kinoshita, M., Saito, A., Fujie, T., Kabata, K., Hara, E., Ono, S., Takeoka, S., Saitoh, D., 2012. An ultrathin poly (L-lactic acid) nanosheet as a burn wound dressing for protection against bacterial infection. Wound Repair Regen. 20, 573–579.
Mohajeri, D., Mesgari, M., Doustar, Y., Nazeri, M., 2011. Comparison of the effect of normal saline and silver sulfadiazine on healing of skin burn wounds in rat: a histopathological study. Middle-East J. Sci. Res. 10 (1), 8–14.
Montes, G.S., Junqueira, L.C.U., 1991. The use of the Picrosirius-Polarization method for the study of the biopathology of collagen. Mem. Inst. Oswaldo Cruz 86 (3), 1–11.
Muzzarelli, R.A.A., 2009. Chitins and chitosans for the repair of wounded skin, nerve, cartilage and bone. Carbohydr. Polym. 76 (2), 167–182.
Neel, E.A.A., Bozec, L., Knowles, L.C., Syed, O., Mudera, V., Day, R., Hyun, J.K., 2012. Collagen – emerging collagen based therapies hit the patient. Adv. Drug Deliv. Rev. 65, 429–456.
Nunes, P.S., Bezerra, M.S., Costa, L.P., Cardoso, J.C., Albuquerque-Júnior, R.L.C., Rodrigues, M.O., Barin, G.B., Silva, F.A., Araújo, A.A.S., 2010. Thermal characterization of usnic acid/collagen-based films. J. Therm. Anal. Calorim. 99, 1011–1014.
Nunes, P.S., Bezerra, M.S., Albuquerque-Júnior, R.L.C., Cavalcante, D.R.R., Dantas, M. D.M., Cardoso, J.C., Souza, J.C.C., Serafini, M.S., Quitans-Júnior, L.J., Bonjardim, L. R., Araújo, A.S.A., 2011. Collagen-Based films containing liposome-loaded usnic acid as dressing for dermal burn healing. J. Biomed. Biotechnol. 12 (1), 9–14.
Papp, A., Valtonen, P., 2006. Tissue substance P leves in acute experimental burns. Burns 32, 842–845.
Prow, T.W., Grice, J.E., Lin, L.L., Faye, R., Butler, M., Becker, W., Wurm, E.M., Yoong, C., Robertson, T.A., Soyer, H.P., Roberts, M.S., 2011. Nanoparticles and microparticles for skin drug delivery. Adv. Drug Deliv. Rev. 63, 470–491.
Raza, K., Singh, B., Lohan, S., Sharma, G., Negi, P., Yachha, Y., Katare, O.P., 2013. Nano-lipoidal carriers of tretinoin with enhanced percutaneous absorption, photostability, biocompatibility and anti-psoriatic activity. Int. J. Pharm. 456, 65–72.
Samy, W., Elgindy, N., El-Gowelll, H.M., 2012. Biopolymeric nifedipine powder for acceleration of wound healing. Int. J. Pharm. 422, 323–331.
Segatore, B., Bellio, P., Setacci, D., Brisdelli, F., Piovano, M., Garbarino, J.A., Nicoletti, M., Amicosante, G., Perilli, M., Celenza, G., 2012. In vitro interaction of usnic acid in combination with antimicrobial agents against methicillin-resistant Staphylococcus aureus clinical isolates determined by FICI and ΔE model methods. Phytomedicine 19, 341–347.
Serafini, M.R., Detoni, C.B., Guterres, S.S., da Silva, G.F., de Souza Araujo, A.A., 2014. Determination of in vitro usnic acid delivery into porcine skin using a HPLC method. J. Chromatogr. Sci. 53, 757–760.
Shvyrkov, M.B., Yanushevich, O.O., 2013. Facial gunshot wound debridement: debridement of facial soft tissue gunshot wounds. J. Cranio Maxill. Surg. 41, 8–16.
Su, -Z.-Q., Mo, Z.-Z., Liao, J.-B., Feng, X.-X., Liang, Y.-Z., Zhang, X., Liu, Y.-H., Chen, X.-Y., Chen, Z.-W., Su, Z.-R., Lai, X.-P., 2014. Usnic acid protects LPS-induced acute lung injury in mice through attenuating inflammatory responses and oxidative stress. Int. Immunopharmacol. 22, 371–378.
Thescher, K., Rocha, T., Cuia, J., Kratza, K., Lendleina, A., Junga, F., 2013. Test system for evaluating the influence of polymer properties onprimary human keratinocytes and fibroblasts in mono- and coculture. J. Biotechnol. 166 (1–2), 58–64.
Velnar, T., Bailey, T., Smrkolj, V., 2009. The wound healing process: an overview of the cellular and molecular mechanisms. J. Int. Med. Res. 37 (5), 1528–1542.
Wanga, T., Zhu, X.K., Xue, X.T., Wu, D.Y., 2012. Hydrogel sheets of chitosan, honey and gelatin as burn wound dressings. Carbohydr. Polym. 88, 75–83.
Yang, Z., Liu, J., Gao, J., Chen, S., Huang, G., 2015. Chitosan coated vancomycin hydrochloride liposomes: characterizations and evaluation. Int. J. Pharm. 495, 508–515.
Yeh, M.-K., Liang, Y.-M., Cheng, K.-M., Dai, N.-T., Liu, C.-C., Young, J.-J., 2011. A novel cell support membrane for skin tissue engineering: gelatin film cross-linked with 2-chloro-1-methylpyridinium iodide. Polymer 52, 996–1003.